

Electronic Supplementary Information for:

Dynamics in the Excited Electronic States of Biphenylene Moieties Embedded in a Framework of Periodic Mesoporous Organosilica Studied by Time-Resolved Diffuse Reflectance and Fluorescence Spectroscopy

*Ken-ichi Yamanaka,^{ab} Tadashi Okada,^{*c} Yasutomo Goto,^{ab} Takao Tani^{ab} and Shinji Inagaki^{*ab}*

^a Toyota Central R&D Labs., Inc., Nagakute, Aichi 480-1192, Japan. E-mail:

inagaki@mosk.tytlabs.co.jp

^b Core Research and Evolutional Science and Technology (CREST), Japan Science and Technology (JST), Kawaguchi, Saitama 332-0012, Japan

^c Toyota Physical & Chemical Research Institute, Nagakute, Aichi 480-1192, Japan

CONTENTS

1. Absorption and fluorescence spectra, and optimized structures of biphenyl and BTEBp
2. Fluorescence excitation spectra of Bp-PMO
3. TDR decay parameters and estimation of α
4. Fluorescence decay curve of BTEBp neat liquid
5. References

1. Absorption and fluorescence spectra and optimized structures of biphenyl and BTEBp

Steady-state absorption and fluorescence spectra of BTEBp in cyclohexane (0.3 mM) and biphenyl in cyclohexane (0.3 mM) are shown in Figure S1. Absorption maxima are observed at 247 nm for biphenyl in cyclohexane and 261 nm for BTEBp in cyclohexane. The absorption band of BTEBp is shifted approximately 14 nm (2170 cm^{-1}) to the longer wavelength and the molecular extinction coefficient is approximately 3.5 times larger than that of biphenyl in cyclohexane. The fluorescence spectrum of biphenyl in cyclohexane under 267 nm excitation shows peaks at 305, 315, 329 (shoulder) nm, while BTEBp in cyclohexane reveals somewhat broader peaks at 311 and 320 nm and a shoulder at 338 nm. The spectrum for BTEBp was shifted approximately 5 nm (630 cm^{-1}), which corresponds to the shift of the absorption band. Biphenyl is known to exist in the planar form in the solid state at room temperature,^{S1-S4} but has a twisted form in the gaseous and solution states.^{S5-S8} A planar structure was suggested for the S_1 state in supersonic free jet^{S7} and in *n*-hexane.^{S8} A large Stokes shift of biphenyl in cyclohexane, calculated to be 7700 cm^{-1} , results from the structural relaxation process from the excited state to the relaxed singlet state.^{S7} In the case of BTEBp in cyclohexane, the Stokes shift was evaluated to be 6200 cm^{-1} , which indicates a similar structural change occurs in the excited state of BTEBp. Molecular orbital (MO) calculations predict a twisted structure in the ground state of BTEBp, as for biphenyl (Figure S2), which implies that the same structural relaxation processes also occur in BTEBp.

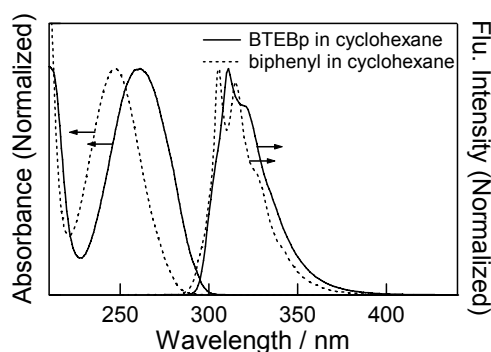


Figure S1. Absorption and fluorescence spectra of BTEBp in cyclohexane and biphenyl in cyclohexane.

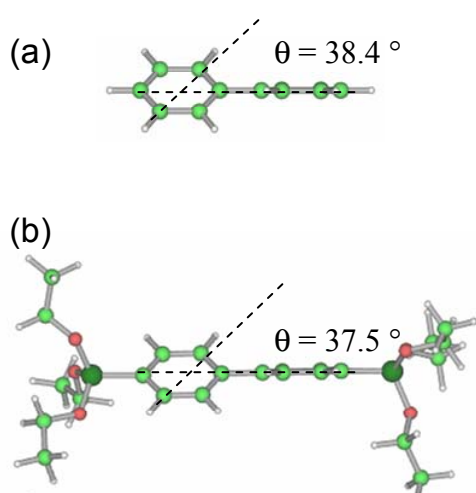


Figure S2. Optimized structures of (a) biphenyl and (b) BTEBp obtained using the *Gaussian 03* density functional theory (DFT) method at the B3LYP/6-31G(d,p) level.^{S9} The dihedral angle of the two phenyl rings is evaluated to be $\theta = 38.4^\circ$ for biphenyl and $\theta = 37.5^\circ$ for BTEBp.

2. Fluorescence excitation spectra of Bp-PMO

Figure S3 shows the fluorescence excitation spectra of a dispersed solution of Bp-PMO particles in 2-MeTHF ($<1 \text{ mg dm}^{-3}$), with a peak at 299 nm and a shoulder at 264 nm. The observed band maximum at 299 nm was considered to be an apparent maximum due to a saturation effect, although the concentration of the dispersed solution was less than 1 mg dm^{-3} , which is the detection limit of the fluorescence spectrometer. The molar extinction coefficient (ϵ) of BTEBp in cyclohexane was evaluated to be $2.6 \times 10^4 \text{ dm}^3 \text{ mol}^{-1} \text{ cm}^{-1}$ at the absorption peak of 261.5 nm. Bp-PMO powder consists of primary particles approximately 300–500 nm in size and the aggregation of several hundred particles is shown in Figure 1a. When the aggregated particle size was assumed to be 10 μm in diameter, the absorbance of Bp-PMO at 295 nm was estimated to be 7.6 using the density of PMO (1.1 g cm^{-3}) and the ϵ of BTEBp in cyclohexane ($1.8 \times 10^3 \text{ dm}^3 \text{ mol}^{-1} \text{ cm}^{-1}$). The absorption band of Bp-PMO is considered to be red shifted, compared to the band of BTEBp, so that the ϵ of Bp-PMO at 295 nm should be larger than the value of BTEBp in cyclohexane ($1.8 \times 10^3 \text{ dm}^3 \text{ mol}^{-1} \text{ cm}^{-1}$).

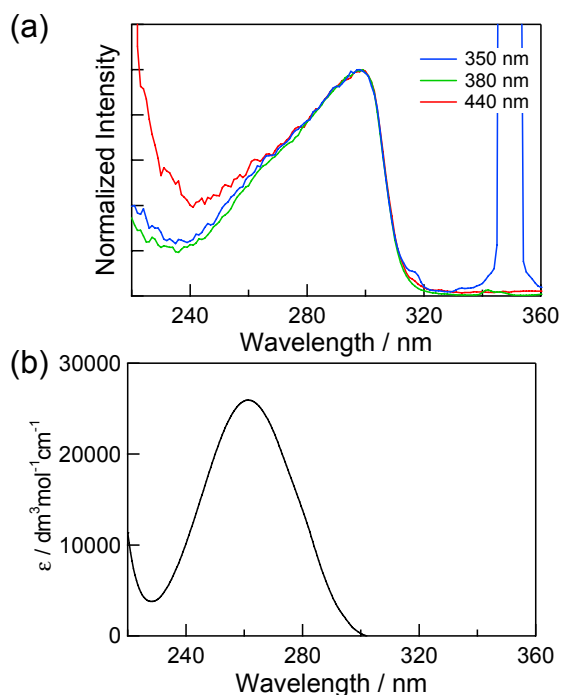


Figure S3. (a) Fluorescence excitation spectra of Bp-PMO dispersed in 2-MeTHF monitored at 350, 380, and 440 nm. (b) Absorption spectrum of BTEBp in cyclohexane at room temperature. Scattered light of 220 nm was overlapped in the short wavelength region of the spectrum monitored at 440 nm (Figure S3a, red line).

3. TDR decay parameters and estimation of α

The TDR decay parameters obtained by global analysis are listed in Table S1. $A_2(\lambda)$ and $A_3(\lambda)$ are given by the following relations:

$$A_2(\lambda) = \varepsilon_\lambda^{S1} FC_0 \alpha k_1 (k_1 - k_2)^{-1} - \varepsilon_\lambda^E FC_0 \alpha k_1 k_2 (k_2 - k_E)^{-1} (k_1 - k_2)^{-1} \quad (S1)$$

$$A_3(\lambda) = \varepsilon_\lambda^{S1} FC_0 (1 - \alpha) k_1 (k_1 - k_3)^{-1} - \varepsilon_\lambda^E FC_0 (1 - \alpha) k_1 k_3 (k_3 - k_E)^{-1} (k_1 - k_3)^{-1} \quad (S2)$$

At $k_E \ll k_2$ and k_3 , $A_2(\lambda)$ and $A_3(\lambda)$ become

$$\begin{aligned} A_2(\lambda) &\approx \varepsilon_\lambda^{S1} FC_0 \alpha k_1 (k_1 - k_2)^{-1} - \varepsilon_\lambda^E FC_0 \alpha k_1 (k_1 - k_2)^{-1} \\ &= \alpha k_1 (k_1 - k_2)^{-1} (\varepsilon_\lambda^{S1} FC_0 - \varepsilon_\lambda^E FC_0) \end{aligned} \quad (S3)$$

$$\begin{aligned} A_3(\lambda) &\approx \varepsilon_\lambda^{S1} FC_0 (1 - \alpha) k_1 (k_1 - k_3)^{-1} - \varepsilon_\lambda^E FC_0 (1 - \alpha) k_1 (k_1 - k_3)^{-1} \\ &= (1 - \alpha) k_1 (k_1 - k_3)^{-1} (\varepsilon_\lambda^{S1} FC_0 - \varepsilon_\lambda^E FC_0) \end{aligned} \quad (S4)$$

The parameter α is given by

$$1/\alpha \approx 1 + A_3(\lambda)(k_1-k_3)A_2(\lambda)^{-1}(k_1-k_2)^{-1} \quad (\text{S5})$$

Table S1. TDR decay parameters obtained by global analysis.

λ / nm	$A_1(\lambda)$	$A_2(\lambda)$	$A_3(\lambda)$	$C(\lambda)$	α
420	0.60	2.11	0.90	1.42	0.68
440	2.23	2.58	1.04	1.20	0.69
460	4.05	2.75	1.10	0.98	0.69
480	4.68	2.82	1.04	0.74	0.71
500	2.98	2.35	0.83	0.56	0.72
520	1.15	1.67	0.65	0.56	0.70
540	0.57	1.22	0.60	0.48	0.65
560	0.28	1.13	0.56	0.35	0.65
580	0.09	1.10	0.57	0.35	0.64
600	0.04	1.14	0.60	0.25	0.63
620	-0.22	1.17	0.68	0.20	0.61
640	0.06	1.28	0.68	0.27	0.63
660	0.02	1.34	0.75	0.35	0.62
680	0.08	1.32	0.79	0.41	0.60
700	0.71	1.24	0.77	0.38	0.59
720	0.41	1.15	0.78	0.44	0.57
740	1.01	0.98	0.70	0.54	0.56
760	0.68	0.79	0.68	0.39	0.51
780	-0.02	0.90	0.47	0.37	0.63

$$\langle \alpha \rangle = 0.64 \pm 0.11$$

4. Fluorescence decay curve of BTEBp neat liquid

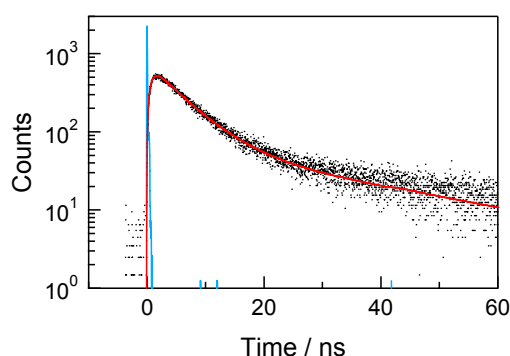


Figure S4. Fluorescence rise and decay curve for the excimer of BTEBp neat liquid at 420 nm at room temperature. The excitation wavelength was 267 nm. The decay curve was deconvoluted as:

$$I(t) = -0.063\exp(-t/0.70\text{ns}) + 0.063\exp(-t/5.3\text{ns}) + 0.062\exp(-t/32\text{ns}).$$

5. References

- (S1) J. Trotter, *Acta Cryst.*, 1961, **14**, 1135.
- (S2) A. Hargreaves and S. H. Rizvi, *Acta Cryst.*, 1962, **15**, 365.
- (S3) G.-P. Charbonneau and Y. Delugeard, *Acta Cryst.*, 1976, **B32**, 1420.
- (S4) G.-P. Charbonneau and Y. Delugeard, *Acta Cryst.*, 1976, **B33**, 1586.
- (S5) H. Suzuki, *Bull. Chem. Soc. Jpn.*, 1959, **32**, 1340.
- (S6) E. D. Schmid and B. Brosa, *J. Chem. Phys.*, 1972, **56**, 6267.
- (S7) J. Murakami, M. Ito and K. Kaya, *J. Chem. Phys.*, 1981, **47**, 6267.
- (S8) C. Kato, H. Hamaguchi and M. Tasumi, *Chem. Phys. Lett.*, 1985, **120**, 183.
- (S9) Gaussian 03, Revision D.02, M. J. Frisch, G. W. Trucks, H. B. Schlegel, G. E. Scuseria, M. A. Robb, J. R. Cheeseman, J. A. Montgomery, Jr., T. Vreven, K. N. Kudin, J. C. Burant, J. M. Millam, S. S. Iyengar, J. Tomasi, V. Barone, B. Mennucci, M. Cossi, G. Scalmani, N. Rega, G. A. Petersson, H. Nakatsuji, M. Hada, M. Ehara, K. Toyota, R. Fukuda, J. Hasegawa, M. Ishida, T. Nakajima, Y. Honda, O. Kitao, H. Nakai, M. Klene, X. Li, J. E. Knox, H. P. Hratchian, J. B. Cross, V. Bakken, C.

Adamo, J. Jaramillo, R. Gomperts, R. E. Stratmann, O. Yazyev, A. J. Austin, R. Cammi, C. Pomelli, J. W. Ochterski, P. Y. Ayala, K. Morokuma, G. A. Voth, P. Salvador, J. J. Dannenberg, V. G. Zakrzewski, S. Dapprich, A. D. Daniels, M. C. Strain, O. Farkas, D. K. Malick, A. D. Rabuck, K. Raghavachari, J. B. Foresman, J. V. Ortiz, Q. Cui, A. G. Baboul, S. Clifford, J. Cioslowski, B. B. Stefanov, G. Liu, A. Liashenko, P. Piskorz, I. Komaromi, R. L. Martin, D. J. Fox, T. Keith, M. A. Al-Laham, C. Y. Peng, A. Nanayakkara, M. Challacombe, P. M. W. Gill, B. Johnson, W. Chen, M. W. Wong, C. Gonzalez and J. A. Pople, Gaussian, Inc., Wallingford CT, 2004.